Communication

Mode Compression Method for Wideband Dipole Antenna by Dual-Point Capacitive Loadings

Hao Li and Yue Li

***Abstract*— In this communication, a dual-mode compression method is proposed for wideband applications of thin dipole antennas. In this method, only two points along the thin dipole antenna are properly found and loaded by two capacitors, lumped or distributed. At these two loading points, there are current nulls of the third mode of the dipole. With two capacitive loadings, an obvious upshifting of the first mode's resonant frequency is observed but with little effects on the third mode. By compressing the first and third modes, an enhancement of the antenna bandwidth is achieved. In addition, a parallel line is used as a transformer for impedance matching. A prototype of the design has been fabricated and tested. The measured results agree well with the simulated ones. In the thin structure of 1.01 × 0.09 λ_0 (λ_0 is the free space wavelength at the center frequency), a wide bandwidth from 1.88 to 3.18 GHz (51.4%) is achieved, performing an omnidirectional radiation pattern with gain of 2.0–4.0 dBi in azimuthal plane.**

***Index Terms*— Broadband antennas, capacitive loading, dipole antennas, multimode resonance.**

I. Introduction

Broadband omnidirectional antennas are required in various kinds of modern communication systems including wireless local area network (WLAN), radio broadcasting, and communication between vehicles. To achieve an omnidirectional radiation pattern, the dipole antenna is usually selected due to its simple structure. Traditional wideband dipoles are designed based on tapered structures or log periodic arrays, indicating large dimensions [1]–[6]. However, thin wire dipoles suffer from high-quality factor (Q-factor) which result in narrow bandwidths [7]. To solve this issue, new methods of enhancing dipole antennas' bandwidths have been proposed and investigated [8]–[17]. One broadband design is using parasitic resonator loadings [8]–[13]. Split-ring resonators [8], dipoles [9], [10], and loops [11] have been utilized to improve the bandwidth of dipole antennas. In particular, a specified design named as the magnetoelectric dipole has attracted a lot of researching interests [12]–[14]. By exciting an electric dipole together with a slot as a magnetic dipole, a wider bandwidth can be obtained. In addition, metamaterials have inspired new approaches in improving bandwidths of thin antennas [15]–[17]. In [15], a dipole antenna based on the mu-negative transmission line (MNG-TL) is presented with a wide bandwidth and a thin structure simultaneously. Periodic overlapped lines are loaded along the dipole. All these approaches involve multiple or periodic structures, which inevitably introduce complicated geometry or large size.

Alternatively, mode compression methods have been employed to enhance the bandwidth [18]–[28] in size-limited designs. Usually, more than one resonant modes are excited, and their resonant frequencies are well designed closer to each other using loaded structures. In [19], a wideband wire dipole operating under the third mode and the fifth mode is designed by loading stubs. Furthermore, the first mode and third mode are used in [20] and [21] to achieve more compact dipoles without losses on bandwidths. Similar methods are proved to be useful on magnetic dipoles, i.e., the narrow slot antennas [22]–[24]. A slot antenna was presented in [22] on which bilateral stub-slots are loaded near the electric field nulls of the third mode. With these loadings, the third resonant mode is moved closer to the first one. In [24], the stubs are replaced by short-circuited lines as two inductive loadings in order to move the first mode upward. All these designs show good performances on bandwidths within thin profiles. However, the widths of all these antennas are larger than the unloaded radiators because of loadings. In addition, several works have been completed on multimode microstrip or cavity antennas. By cutting slots on the patches [25]–[28] or cavities [29], the bandwidths are obviously enhanced. In these designs, the slots are loaded within the original structures to achieve smaller dimensions.

Inspired by these results, a dual-mode thin dipole loaded with two interdigital capacitors [30] is first presented here with a broadband performance and stable radiation pattern. On a thin dipole operating under first mode and third mode, two capacitive loadings at two points are positioned near the current nulls of the third mode. By loading these two elements, only the resonant frequency of the first mode is shifted to higher bands. As a result, the first and third modes are compressed, generating a wide bandwidth under dual-mode resonance. A prototype of the design has been fabricated and measured to verify the proposed method. With both the dipole and the feeding parallel line placed in a size of 1.01 × 0.09 λ_0, the antenna shows a −10 dB impedance bandwidth of 56.49% from 1.88 to 3.36 GHz. Meanwhile, stable omnidirectional radiation patterns in azimuthal plane are also achieved from 1.85 to 3.18 GHz in which the gain varies from 2.0 to 4.0 dBi.

II. Antenna Design and Operating Principles

The schematic and geometry structure of the proposed antenna is shown in Fig. 1. The antenna is designed based on a theoretical model of a thin dipole loaded with two lumped capacitors, as depicted in Fig. 1(a). The geometry of the antenna is shown in Fig. 1(b). The thin dipole is printed on the top layer of a F4B substrate with a permittivity of 2.65 and loss tangent of 0.002. Each arm of the dipole is loaded by an interdigital capacitor at the place of one third of the arm's length. The structure of the capacitive loading is clearly seen in Fig. 1(c), with small stubs on both sides. The geometry parameters are chosen carefully to achieve a capacitance of 0.05 pF. In order to match the input impedance of the dipole to 50 Ω, a parallel line is

Manuscript received November 10, 2019; revised January 23, 2020; accepted January 27, 2020. Date of publication February 14, 2020; date of current version August 4, 2020. This work was supported in part by the Natural Science Foundation of Beijing Manipulate under Contract 4182029, in part by the Tsinghua University Initiative Scientific Research Program under Contract 2019Z08QCX16, and in part by the Youth Top Program of Beijing Outstanding Talent Funding Project. (*Corresponding author: Yue Li.*)

The authors are with the Department of Electronic Engineering, Tsinghua University, Beijing 100084, China, and also with the Beijing National Research Center for Information Science and Technology, Tsinghua University, Beijing 100084, China (e-mail: lyee@tsinghua.edu.cn).

Color versions of one or more of the figures in this communication are available online at http://ieeexplore.ieee.org.

Digital Object Identifier 10.1109/TAP.2020.2972642

TABLE I
DETAILED DIMENSIONS

Parameter	Value (mm)	Parameter	Value (mm)	Parameter	Value (mm)
L_1	23.0	L_2	36.0	L_3	8.0
L_4	0.5	W_1	3.5	W_2	1.0
W_3	0.4	W_4	0.8	L_S	130.0
W_S	19.7	d	1.0	g	1.0
H	1.0				

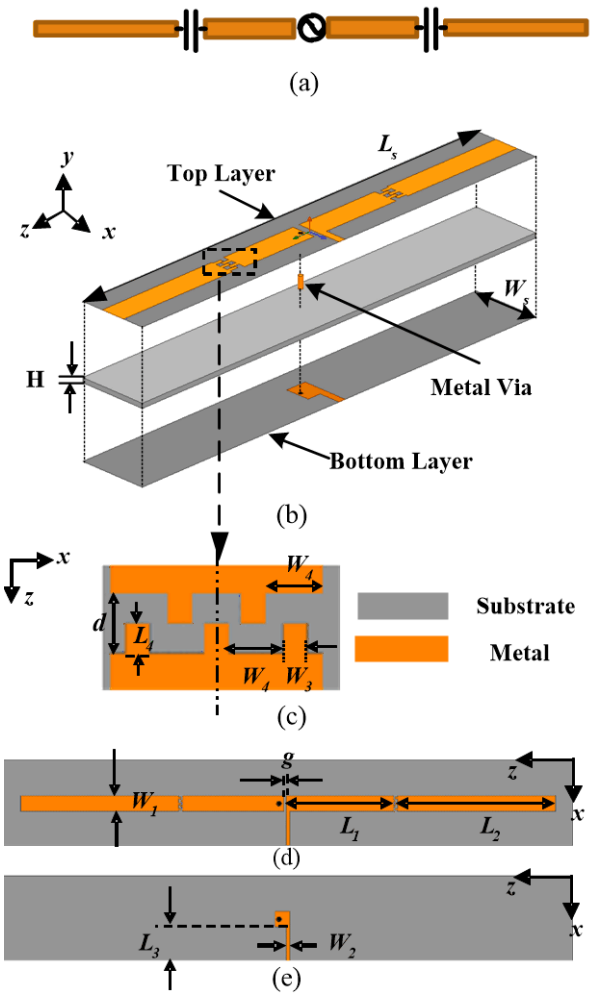

Fig. 1. Configuration of the proposed antenna: (a) theoretical model, (b) perspective view, (c) zoomed-in view of the distributed capacitor loading, (d) front, and (e) back views.

used along x-axis, consisting of two metal wires separated by the substrate. The top one is connected to one arm of the dipole and that on the bottom is connected to the other arm through a metal via. The detailed dimensions are listed in Table I.

To illustrate the operating principles of the antenna, the theoretical model in Fig. 1(a) is first investigated. In this model, the length and loading positions are kept the same with the actual design in Fig. 1(b). Simulations have been launched on the dipole using HFSS [31] to study the impedance properties when the dipole is loaded with different capacitors. The simulated S-parameters and input reactance are all shown in Fig. 2. According to Fig. 2(a), the resonant frequency

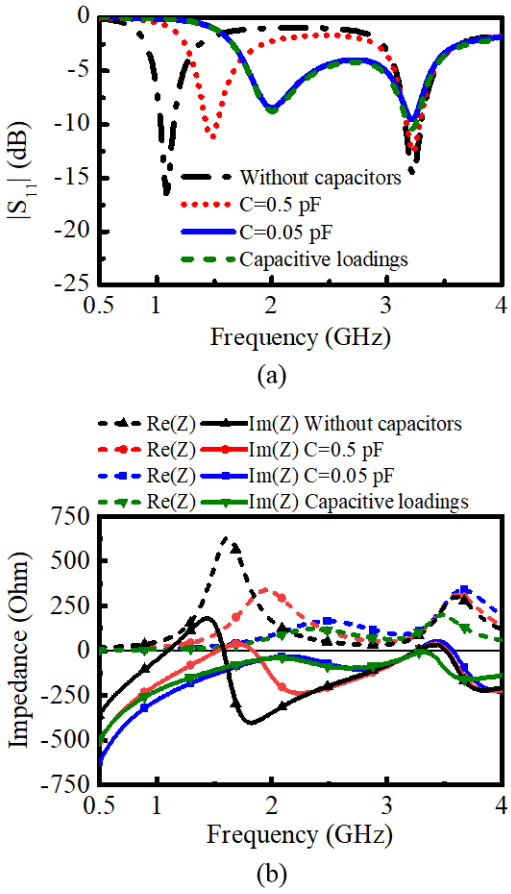

Fig. 2. Simulated (a) S-parameters and (b) input impedance of the schematic dipole model with different loaded capacitors or capacitive loadings.

of the first mode and the third mode of an unloaded dipole is simulated to be 1.08 and 3.24 GHz. As the capacitance decreases, the first resonance moves to higher frequencies, whereas the third one remains at 3.24 GHz without obvious changes. In other words, loading two capacitors with smaller capacitances can compress the resonant frequencies of the two modes closer to each other. Similar results can be concluded from the input reactance shown in Fig. 2(c). Moreover, comparisons on S-parameters and input reactance have been also made using lumped capacitors of 0.05 pF and the capacitive loadings in the actual designs. It can be seen from Fig. 2(a) that the S-parameters of these two situations match perfectly with each other.

This phenomenon can be explained by the different effects introduced by the loading capacitors on the first and the third modes. It is known that the impedance characteristics of each mode of the dipole can be described using a serial LC resonance circuit consisting of a capacitor, an inductor, and a radiating resistor. When the first mode is excited, strong currents are flowing along the capacitors, so that a capacitor is added in series to the LC circuit. This additional serial capacitor reduces the total capacitance of the LC circuit, resulting in an increase in the resonant frequency of the first mode. However, this is not compliant to the third mode. In this case, the currents flowing through the capacitor are very weak, so the added capacitance is smaller enough to be neglected, thus having little effects on the resonant frequency of the third mode. Therefore, these two modes are compressed together by loading capacitors. To further understand the working principle of the antenna, the current distributions at different frequencies are depicted in Fig. 3. It can be observed that only the first mode is excited at 2 GHz since the currents on the dipole present

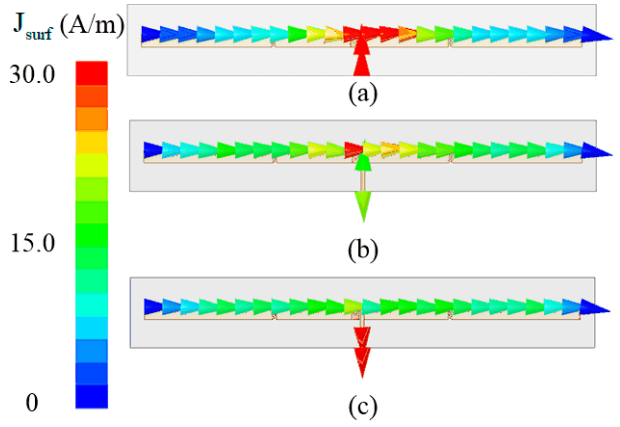

Fig. 3. Surface current distributions on the dipole at (a) 2 GHz, (b) 2.5 GHz, and (c) 3 GHz.

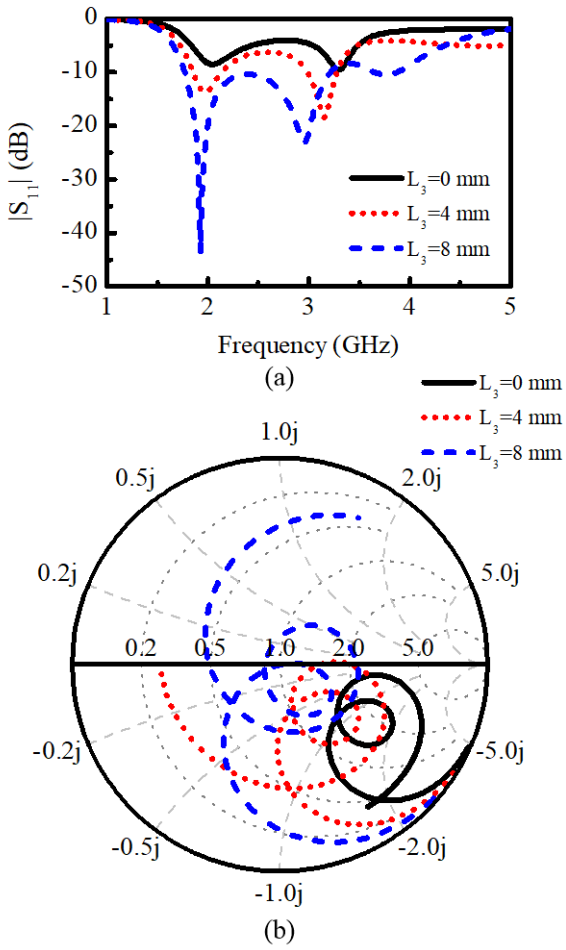

Fig. 4. Impedance matching using the parallel line: (a) S-parameters and (b) Smith chart with respect to the lengths of the parallel line.

a sinusoidal distribution. At 2.5 and 3 GHz, the first and the third modes both exist to perform a uniform current distribution. It can also be seen that the third mode is stronger at 3 GHz for the current at the center is weaker than that at 2 or 2.5 GHz.

Next, for impedance matching, a parallel line with 100 Ω characteristic impedance has been used as an impedance transformer. Fig. 4 shows the parametric study on the impedance properties with

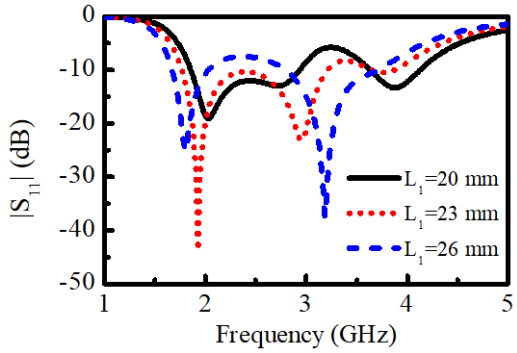

Fig. 5. Variation in the S-parameters with respect to the positions of the capacitive loadings.

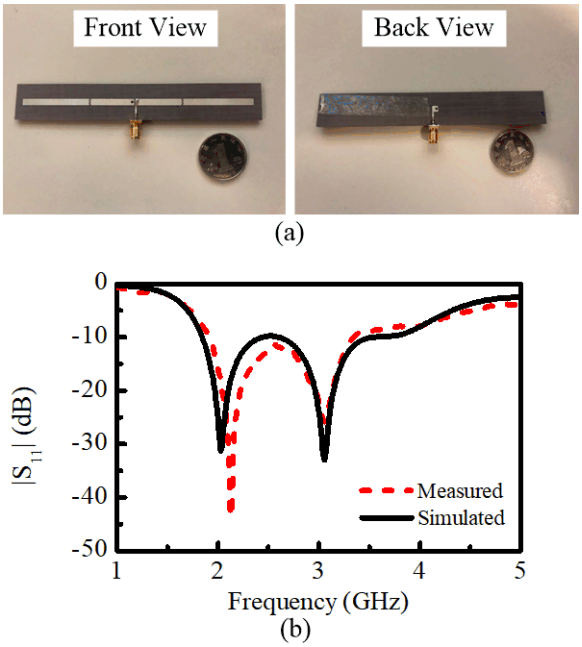

Fig. 6. Antenna measurements: (a) fabricated prototype from the front and back views and (b) simulated and measured S-parameters.

variation in the length of the parallel line. The reflection coefficient is suppressed under −10 dB when L_3 is optimized to be 8 mm according to Fig. 4(a). These results are corresponding to the Smith chart shown in Fig. 4(b). It can be seen that as the length increases, the impedance curve is rotating around the 100 Ω point in clockwise. When L_3 reaches 8 mm, the input impedances are transformed close to 50 Ω within a wide frequency range. In Fig. 5, various S-parameters with respect to the positions of the capacitive loadings are plotted. Here the sum of L_1 and L_2 is kept to be 59 mm, so that changing L_1 does not affect the total length of the dipole. When the two capacitive loadings are placed exactly at the one-third point of the dipole, i.e., $L_1 = 20$ mm, the maximum compression is obtained from the first and the third modes. As L_1 increases and L_2 decreases, the resonant frequencies of these two modes are separated from each other. This phenomenon is because the frequency shift of each resonant mode depends on the current intensity flowing along the capacitive loadings. When the loadings are moved closer to the edge of the dipole, the currents of the first mode at the loading point become weaker, so that the frequency shift of the first mode is smaller. Moreover, the currents of the third mode at the loading point are not zero, so that the third mode is also slightly upshifted. By optimizing

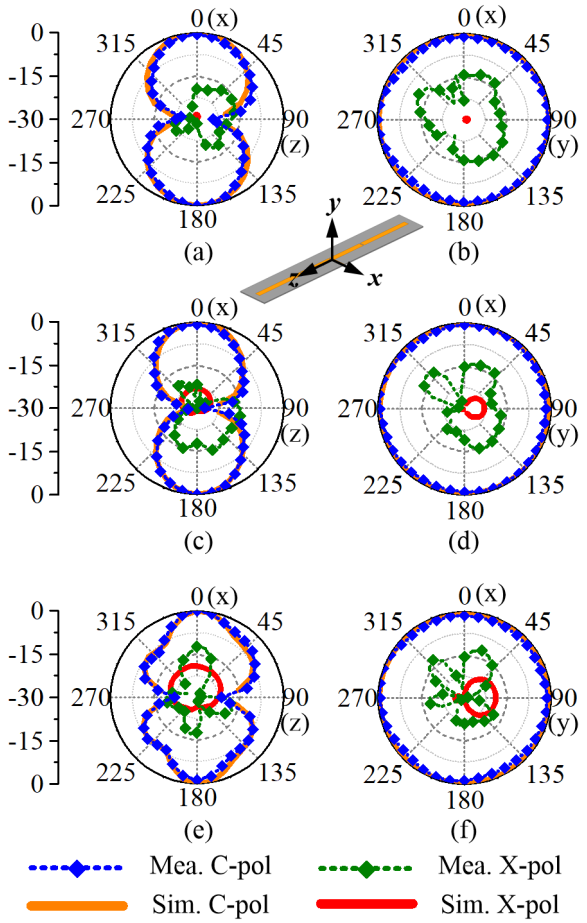

Fig. 7. Normalized simulated and measured radiation patterns at: (a) 2 GHz, elevation (*XZ*) plane, (b) 2 GHz, azimuthal (*XY*) plane, (c) 2.5 GHz, elevation (*XZ*) plane, (d) 2.5 GHz, azimuthal (*XY*) plane, (e) 3 GHz, elevation (*XZ*) plane, and (f) 3 GHz, azimuthal (*XY*) plane.

the positions of the capacitive loadings, the bandwidth of the antenna is further widened.

III. Antenna Fabrication and Measurement Results

To validate the design, a prototype has been fabricated and tested. A subminiature-A (SMA) connector is soldered at the end of the parallel line for connection to a 50 Ω coaxial cable, as shown in Fig. 6(a). The antenna is measured using the N9917A vector network analyzer. As depicted in Fig. 6(b), the measured $|S_{11}|$ agrees well with the simulated one, with −10 dB impedance bandwidth of 1.48 GHz (56.5%) from 1.88 to 3.36 GHz.

The radiation patterns and gains of the antenna are also measured in an anechoic chamber. Fig. 7 shows the normalized radiation patterns at different frequencies in both azimuthal and elevation planes. The measured results agree with simulations except for slightly higher cross-polarization at 2 GHz. The antenna is with an omnidirectional radiation pattern in the azimuthal plane. At 2 and 2.5 GHz, the radiation pattern in the elevation plane is a bidirectional ∞-shaped pattern. At 3 GHz, the third mode of the dipole is dominant with small sidelobe in the elevation plane. The measured and simulated gains of the fabricated prototype are shown in Fig. 8. The antenna exhibits a gain bandwidth from 1.85 to 3.18 GHz and a stable broadside radiation pattern and gain fluctuation of 2 dB within its impedance bandwidth. Good agreements are reached between the simulations and measurements.

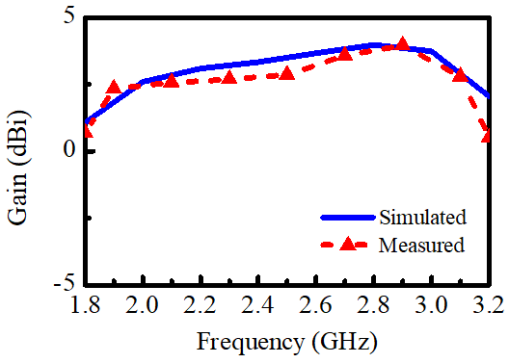

Fig. 8. Simulated and measured gains of the proposed antenna.

TABLE II
Comparison Among the Proposed Design and Other Related Antennas

Reference	Antenna Type	Bandwidth (%)	Effective Size (λ_0^2)	Total Size (λ_0^2)
[10]	Dipole	63.8	0.56×0.16	0.56×0.16
[11]	Dipole & Loop	44.2	0.49×0.09	0.63×0.32
[15]	Dipole	59.0	1.31×0.12	1.31×0.16
[19]	Dipole	11.2	0.83×0.60	1.04×0.83
[20]	Dipole	27.8	0.42×0.10	0.45×0.17
[21]	Dipole	49.7	0.59×0.36	0.59×0.36
[22]	Slot	21.0	0.70×0.17	1.32×1.32
[23]	Slot	31.5	0.72×0.35	1.32×1.32
[24]	Slot	39.7	1.18×0.80	1.76×1.76
[29]	Cavity	25.0	0.55×0.55	0.55×0.55
[32]	Cavity	9.1	1.58×0.19	2.13×0.66
Proposed	**Dipole**	**51.4**	**1.01×0.09**	**1.08×0.16**

Table II lists the comparisons made with related works [10], [11], [15], [19]–[24], [29], and [32]. Unprinted substrates, ground planes with no slots, and 50 Ω microstrip lines are omitted when comparing the effective sizes. It can be concluded from the table that the proposed dual-mode compression method has the narrowest width even though the bandwidth is wider than most of the designs. A wider bandwidth than [11] is achieved with the same width of 0.09 λ_0. Without using parasitic stubs or loops, the antenna achieves a thin profile compared with dipoles in [10], [19], [20], and [21].

IV. Conclusion

In this communication, a dual-mode compression method using two compact capacitive loadings has been first proposed to enhance the bandwidth of thin dipole antennas. In this method, two interdigital capacitors are loaded near the current nulls of the dipole's third mode. Using this dual-point loading, the resonant frequency of the first mode has been moved to higher bands with little effects on the third one, producing a compression of two modes and a wideband property. This method has been proven to work using either lumped or distributed capacitive loadings, and a broadband dipole antenna has been designed, fabricated, and measured. A good performance including an effective bandwidth of 51.4% (1.88–3.18 GHz) and omnidirectional radiation pattern is obtained within a thin size of 1.01 × 0.09 λ_0.

REFERENCES

[1] J. Liu, K. P. Esselle, and S. Zhong, "A printed extremely wideband antenna for multi-band wireless systems," in *Proc. IEEE Antennas Propag. Soc. Int. Symp.*, Toronto, ON, Canada, Jul. 2010, pp. 1–4.

[2] J. Mruk, Z. Hongyu, M. Uhm, Y. Saito, and D. Filipovic, "Wideband mm-wave log-periodic antennas," in *Proc. 3rd Eur. Conf. Antennas Propag.*, Berlin, Germany, 2009, pp. 2584–2587.

[3] S. Choudhury, A. Mohan, and D. Guha, "A new printed log periodic antenna using SIW concept," in *Proc. IEEE Indian Conf. Antennas Propag. (InCAP)*, Hyderabad, India, Dec. 2018, pp. 1–3.

[4] S. M. Moghaddam, J. Yang, A. A. Glazunov, and A. U. Zaman, "A planar single-polarized ultra-wideband antenna element for millimeter-wave phased array," in *Proc. Int. Symp. Antennas Propag. (ISAP)*, Busan, South Korea, 2018, pp. 1–2.

[5] A. A. Omar and Z. Shen, "Compact and wideband dipole antennas," in *Proc. IEEE-APS Topical Conf. Antennas Propag. Wireless Commun. (APWC)*, Granada, Spain, Sep. 2019, pp. 1–3.

[6] W. D. Ake, M. Pour, and A. Mehrabani, "Asymmetric half-bowtie antennas with tilted beam patterns," *IEEE Trans. Antennas Propag.*, vol. 67, no. 2, pp. 738–744, Feb. 2019.

[7] G. A. E. Vandenbosch, "Reactive energies, impedance, and Q factor of radiating structures," *IEEE Trans. Antennas Propag.*, vol. 58, no. 4, pp. 1112–1127, Apr. 2010.

[8] K. E. Kedze, H. Wang, and I. Park, "Compact broadband omnidirectional radiation pattern printed dipole antenna incorporated with split-ring resonators," *IEEE Access*, vol. 6, pp. 49537–49545, 2018.

[9] R. Wu and Q.-X. Chu, "Resonator-loaded broadband antenna for LTE700/GSM850/GSM900 base stations," *IEEE Antennas Wireless Propag. Lett.*, vol. 16, pp. 501–504, 2017.

[10] H.-T. Hsu and T.-J. Huang, "Generic dipole-based antenna-featuring dual-band and wideband modes of operation," *IET Microw., Antennas Propag.*, vol. 6, no. 15, pp. 1623–1628, Dec. 2012.

[11] D. Wen, Y. Hao, H. Wang, and H. Zhou, "Design of a wideband antenna with stable omnidirectional radiation pattern using the theory of characteristic modes," *IEEE Trans. Antennas Propag.*, vol. 65, no. 5, pp. 2671–2676, May 2017.

[12] K.-M. Luk and B. Wu, "The magnetoelectric dipole—A wideband antenna for base stations in mobile communications," *Proc. IEEE*, vol. 100, no. 7, pp. 2297–2307, Jul. 2012.

[13] S. J. Yang, Y. M. Pan, Y. Zhang, Y. Gao, and X. Y. Zhang, "Low-profile dual-polarized filtering magneto-electric dipole antenna for 5G applications," *IEEE Trans. Antennas Propag.*, vol. 67, no. 10, pp. 6235–6243, Oct. 2019.

[14] S. Ahdi Rezaeieh and A. M. Abbosh, "Pattern-reconfigurable magnetoelectric antenna utilizing asymmetrical dipole arms," *IEEE Antennas Wireless Propag. Lett.*, vol. 18, no. 4, pp. 688–692, Apr. 2019.

[15] K. Wei, Z. Zhang, Z. Feng, and M. F. Iskander, "A wideband MNG-TL dipole antenna with stable radiation patterns," *IEEE Trans. Antennas Propag.*, vol. 61, no. 5, pp. 2418–2424, May 2013.

[16] H. Sun, C. Ding, Y. J. Guo, and R. Mittra, "A wideband dipole antenna based on a non-uniformly segmented structure," in *Proc. 11th Eur. Conf. Antennas Propag. (EUCAP)*, Mar. 2017, pp. 3572–3574.

[17] X. Jia and D. Piao, "A wideband segmented line dipole antenna with stable radiation patterns," in *Proc. 11th Int. Symp. Antennas, Propag. EM Theory (ISAPE)*, Oct. 2016, pp. 22–24.

[18] W.-J. Lu, J. Yu, and L. Zhu, "On the multi-resonant antennas: Theory, history and new development," *Int. J. RF Microw. Comp.-Aided Eng.*, vol. 29, e21703, 2019.

[19] Y. Luo, Z. N. Chen, and K. Ma, "Enhanced bandwidth and directivity of a dual-mode compressed high-order mode stub-loaded dipole using characteristic mode analysis," *IEEE Trans. Antennas Propag.*, vol. 67, no. 3, pp. 1922–1925, Mar. 2019.

[20] W. Zhang, Y. Li, Z. Zhou, and Z. Zhang, "Dual-mode compression of dipole antenna by loading electrically small loop resonator," *IEEE Trans. Antennas Propag.*, to be published.

[21] W.-J. Lu, L. Zhu, K. W. Tam, and H.-B. Zhu, "Wideband dipole antenna using multi-mode resonance concept," *Int. J. Microw. Wireless Technol.*, vol. 9, no. 2, pp. 365–371, Mar. 2017.

[22] W.-J. Lu and L. Zhu, "A novel wideband slotline antenna with dual resonances: Principle and design approach," *IEEE Antennas Wireless Propag. Lett.*, vol. 14, pp. 795–798, 2015.

[23] W.-J. Lu and L. Zhu, "Wideband stub-loaded slotline antennas under multi-mode resonance operation," *IEEE Trans. Antennas Propag.*, vol. 63, no. 2, pp. 818–823, Feb. 2015.

[24] W.-J. Lu and L. Zhu, "Planar dual-mode wideband antenna using short-circuited-strips loaded slotline radiator: Operation principle, design, and validation," *Int. J. RF Microw. Comput.-Aided Eng.*, vol. 25, no. 7, pp. 573–581, Sep. 2015.

[25] N.-W. Liu, L. Zhu, G. Fu, and Y. Liu, "A low profile shorted-patch antenna with enhanced bandwidth and reduced H-plane cross-polarization," *IEEE Trans. Antennas Propag.*, vol. 66, no. 10, pp. 5602–5607, Oct. 2018.

[26] N. Liu, L. Zhu, and W. Choi, "A Differential-fed microstrip patch antenna with bandwidth enhancement under operation of TM10 and TM30 modes," *IEEE Trans. Antennas Propag.*, vol. 65, no. 4, pp. 1607–1614, Apr. 2017.

[27] W. Liu, Z. N. Chen, and X. Qing, "Metamaterial-based low-profile broadband aperture-coupled grid-slotted patch antenna," *IEEE Trans. Antennas Propag.*, vol. 63, no. 7, pp. 3325–3329, Jul. 2015.

[28] W. Sun, Y. Li, Z. Zhang, and Z. Feng, "Broadband and low-profile microstrip antenna using strip-slot hybrid structure," *IEEE Antennas Wireless Propag. Lett.*, vol. 16, pp. 3118–3121, 2017.

[29] W.-J. Lu, X.-Q. Li, Q. Li, and L. Zhu, "Generalized design approach to compact wideband multi-resonant patch antennas," *Int. J. RF Microw. Comput.-Aided Eng.*, vol. 28, no. 8, Oct. 2018, Art. no. e21481.

[30] G. Alley, "Interdigital capacitors and their application to lumped-element microwave integrated circuits," *IEEE Trans. Microw. Theory Techn.*, vol. 18, no. 12, pp. 1028–1033, Dec. 1970.

[31] *ANSYS Corporation HFSS*. Accessed: 2020. [Online]. Available: https://www.ansys.com/products/electronics/ansys-hfss

[32] Y. Shi and J. Liu, "Investigation of a via-loaded microstrip magnetic dipole antenna with enhanced bandwidth and gain," *IEEE Trans. Antennas Propag.*, vol. 67, no. 7, pp. 4836–4841, Jul. 2019.